Acta Crystallographica Section F
Structural Biology and Crystallization Communications
ISSN 1744-3091

Crystallization and preliminary crystallographic analysis of the complex between triiodothyronine and the *bb′* fragment of rat protein disulfide isomerase

Shoko Hashimoto,[a] Len Ito,[b] Masaki Okumura,[a] Tomohisa Shibano,[a] Marina Nawata,[a] Takashi Kumasaka,[b] Hiroshi Yamaguchi[a]* and Susumu Imaoka[a]

[a]School of Science and Technology, Kwansei Gakuin University, 2-1 Gakuen, Sanda, Hyogo 669-1337, Japan, and [b]Synchrotron Radiation Research Institute (SPring-8), 1-1-1 Kouto, Sayo, Hyogo 679-5198, Japan

Correspondence e-mail: hiroshi@kwansei.ac.jp

Received 1 October 2011
Accepted 19 February 2012

Protein disulfide isomerase (PDI) is a multifunctional protein that catalyzes the formation of a disulfide bond in nascent and misfolded proteins and is also known to bind to the thyroid hormone triiodothyronine (T3). When T3 is bound to PDI its catalytic activity is inhibited, but the biological function of this binding is not well understood. In previous studies, it was found that T3 binds to the *bb′* fragment of PDI. Therefore, to clarify the structure of the complex consisting of PDI bound to T3, a crystallographic analysis of the three-dimensional structure of the T3–rat PDI *bb′* complex was performed. Native *bb′* crystals and T3–*bb′* complex crystals were both obtained using the hanging-drop vapour-diffusion technique with 1.6 *M* trisodium citrate pH 6.2 as a precipitant. The space group of the native *bb′* crystals was found to be *C*222, with unit-cell parameters $a = 94.8$, $b = 114.9$, $c = 182.9$ Å, while the space group of the T3–*bb′* complex crystals was $P2_12_12_1$, with unit-cell parameters $a = 99.9$, $b = 184.5$, $c = 232.2$ Å. Diffraction data for the native and complex crystals were collected to resolutions of 3.06 and 3.00 Å, respectively.

1. Introduction

Protein disulfide isomerase (PDI) is a key enzyme involved in the formation of correct disulfide bonds in nascent or misfolded proteins in the endoplasmic reticulum. PDI consists of four thioredoxin-like domains: *a*, *b*, *b′* and *a′*. The *a* and *a′* domains contain the catalytically active Cys-Gly-His-Cys site, while the *b* and *b′* domains are redox-inactive but play an important role in substrate binding (Darby & Creighton, 1995*a*,*b*). PDI catalyzes the formation, reduction and isomerization of disulfide bonds *via* cysteine residues in its catalytically active sites.

In a previous study, we isolated PDI from the synaptosome fraction of rat brain as a bisphenol A [BPA; 2,2′-bis(4-hydroxyphenyl)-propane] binding protein (Hiroi *et al.*, 2006). BPA is an epoxy-resin monomer and is contained in a variety of industrial chemical products. BPA has also been reported to be an endocrine-disrupting chemical and exhibits oestrogen-like effects and neural toxicity (Obata & Kubota, 2000; Suzuki *et al.*, 2003). BPA binds competitively to PDI with not only oestrogen (E2) but also triiodothyronine (T3). Both BPA and T3 inhibit the catalytic activity of PDI (Hiroi *et al.*, 2006). The K_d of recombinant rat PDI for [^{3}H]-BPA has been determined to be 22.6 ± 6.6 µ*M* (Hiroi *et al.*, 2006) and that for T3 has been reported to be 4.3 µ*M* (Primm & Gilbert, 2001). Moreover, we investigated the structure that is required for binding activity and the inhibitory effect on the catalytic activity using six BPA derivatives and found the hydroxyl group(s) of the benzene ring(s) in BPA to be important (Hashimoto *et al.*, 2008). T3 also has a phenol structure and its K_d is lower than that of BPA. Primm & Gilbert (2001) proposed that the high-capacity low-affinity hormone sites of PDI serve as hormone reservoirs to buffer the hormone concentration in cells. In a previous study, we showed that overexpression of PDI in GH3 cells reduces the expression of growth hormone, which is induced by T3 *via* a thyroid hormone receptor (Okada *et al.*, 2007). However, the biological reason for the binding of PDI to the hormone remains unclear.

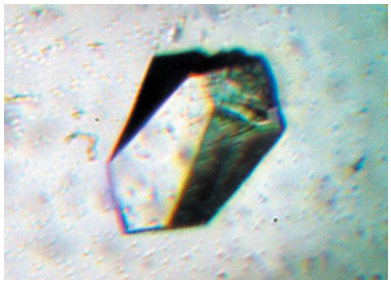

We recently reported that BPA and T3 bind to the *bb′* fragment of PDI. Since the *b′* domain contains the substrate-binding region, it is possible that binding of T3 or BPA inhibits substrate recognition by the *b′* domain, which would lead to the inhibitory effects observed on the catalytic activity of PDI. The structures of the individual *a*, *b* and *b′* domains of human PDI have been determined by NMR spectroscopy or crystal structure analysis and these studies revealed that these domains adopt the thioredoxin fold (Kemmink *et al.*, 1995, 1999; Nguyen *et al.*, 2008). In addition, the crystal structure of yeast PDI has been solved and the results indicated that the four thioredoxin domains of yeast PDI form a twisted U shape (Tian *et al.*, 2006); mammalian PDI has not yet been crystallized. Fu *et al.* (2011) reported that pancreas-specific protein disulfide isomerase (PDIp) binds to E2 *via* the *bb′* domain and that both the *b* and *b′* domains are required for the binding of E2 to PDIp.

Therefore, in order to better understand the structure of the complex formed when PDI binds to T3 or BPA, we performed crystal structural analyses of the *bb′* fragment and its T3 or BPA complex. The clarification of the binding mode between T3 or BPA and PDI may provide useful information for understanding the mechanism involved in the inhibition of the catalytic activity of PDI by T3 or BPA and the physiological significance of T3 binding to PDI. Here, we report preliminary X-ray studies of the complex between T3 and rat PDI *bb′* fragment.

2. Methods

2.1. Expression of the *bb′* fragment of rat PDI in *Escherichia coli* and its purification

Rat PDI cDNA was cloned as described previously (Hiroi *et al.*, 2006). The polymerase chain reaction (PCR) of the *bb′* fragment (amino acids 120–353 of PDI; GenBank Accession No. NM_012998) was performed with the forward primer 5′-AA**GGATCC**GCTGGCAGGGAAGCTGAC-3′ (the *Bam*HI site is shown in bold) and the reverse primer 5′-TT**GTCGAC**CTACAGGATCTTGCCCTCCA-3′ (the *Sal*I site is shown in bold and the stop codon is underlined) using full-length PDI cDNA as a template (Hiroi *et al.*, 2006). PCR was performed with High-Fidelity DNA Polymerase and consisted of denaturation at 367 K for 2 min followed by 30 cycles of 367 K for 30 s, 328 K for 30 s and 345 K for 1 min. The cDNA of the *bb′* fragment was cut with *Bam*HI and *Sal*I and ligated into a pQE-80L vector (Qiagen, Valencia, California, USA). The protein contains a sequence derived from the pQE-80L vector and six histidines (MRGSHHHHHHGS) at the N-terminus; the expressed protein therefore contains 247 amino-acid residues with a molecular weight of 27.7 kDa.

BL21 *E. coli* cells (Novagen, Madison, Wisconsin, USA) transformed with pQE-80L encoding the histidine-tagged *bb′* fragment of rat PDI were grown at 310 K in 2× yeast extract/tryptone-rich medium (1 l) containing 0.1 mg ml^{-1} ampicillin. Protein expression was induced by adding 1.0 m*M* isopropyl *β*-D-1-thiogalactopyranoside. After additional cultivation for 6 h, the *E. coli* cells were harvested and suspended in lysis buffer (50 m*M* NaH_2PO_4 pH 7.5 containing 300 m*M* NaCl, 1.0 mg ml^{-1} lysozyme and 20 m*M* imidazole). The *E. coli* cells were sonicated and the resulting lysate was centrifuged at 50 000*g* for 30 min. The supernatant was loaded onto a 10 ml Ni–NTA agarose column (Qiagen) equilibrated with lysis buffer and the protein was eluted with lysis buffer containing 250 m*M* imidazole. The eluted protein was then further purified by passage through a 20 ml DE52 (Whatman) ion-exchange column equilibrated with 50 m*M* Tris–HCl pH 7.5 containing 150 m*M* NaCl and proteins were eluted with a salt gradient from 150 to 400 m*M* NaCl in 50 m*M* Tris–HCl pH 7.5. Around 25 mg *bb′* fragment was obtained from 1 l culture medium.

2.2. Crystallization of the *bb′* fragment

The purified *bb′* fragment was concentrated to 7.0 mg ml^{-1}. Crystallization conditions were initially screened using Crystal Screen, Crystal Screen 2 (Hampton Research) and Wizard I and II (Emerald BioStructures) by the hanging-drop vapour-diffusion method at 277 and 293 K. To optimize the initial crystallization conditions, the concentration of protein (3.5, 7.0 or 10 mg ml^{-1}), the reservoir solution and the pH of the reservoir (6.2, 7.5 and 8.5) were examined. The best conditions for crystallization were determined to be as follows: hanging drops were produced by mixing 2.0 µl 7.0 mg ml^{-1} *bb′* fragment solution and 2.0 µl precipitant solution (1.6 *M* trisodium citrate dehydrate pH 6.2). The mixture was equilibrated against 500 µl reservoir solution consisting of 1.6 *M* trisodium citrate dehydrate pH 6.2 at 293 K. Crystals of the T3–*bb′* fragment complex were obtained by cocrystallization under the same conditions as were used for the native crystals. Before preparing the droplets, 100 µ*M* T3 was mixed with the *bb′* fragment at 7 mg ml^{-1} in 50 m*M* Tris–HCl pH 7.5. The native and complex crystals both grew within one week (Fig. 1).

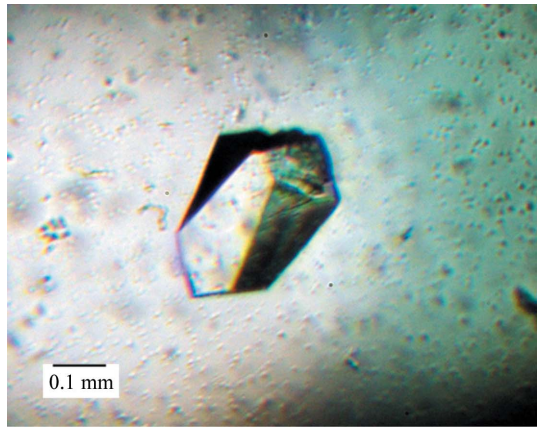

(*a*)

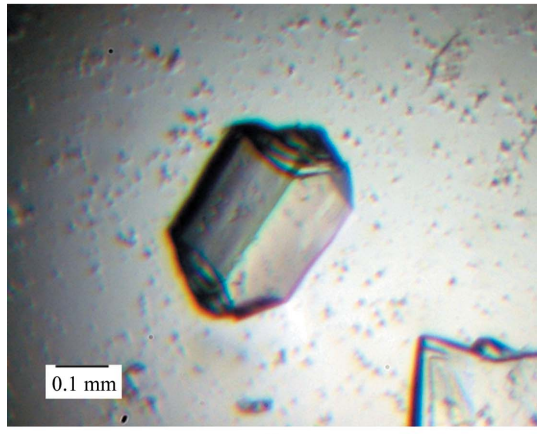

(*b*)

Figure 1
Typical appearance of crystals in hanging drops. (*a*) Crystals of the *bb′* fragment were formed in the presence of 1.6 *M* sodium citrate pH 6.2 using 7.0 mg ml^{-1} *bb′* fragment solution at 293 K. (*b*) Crystals of the T3–*bb′* complex were produced in the presence of 1.6 *M* sodium citrate pH 6.2 using 7.0 mg ml^{-1} *bb′* fragment solution containing 100 µ*M* T3. Crystals were grown under the same conditions as native *bb′*. Both crystals grew within one week and reached maximum dimensions of at least 0.2 × 0.2 × 0.1 mm.

Table 1
Data-collection and diffraction data statistics.

Values in parentheses are for the highest resolution shell.

	Native	Complex
Beamline	BL38B1, SPring-8	BL38B1, SPring-8
Detector	ADSC Q315	ADSC Q315
Wavelength (Å)	1.000	1.000
Crystal-to-detector distance (mm)	380	360
Oscillation angle (°)	0.5	0.5
Total oscillation range (°)	180	180
Space group	$C222$	$P2_12_12_1$
Unit-cell parameters		
a (Å)	94.81	99.92
b (Å)	114.90	184.52
c (Å)	182.88	232.19
Resolution (Å)	40–3.06 (3.17–3.06)	40–3.00 (3.11–3.00)
Multiplicity	3.8 (3.8)	3.5 (3.3)
Completeness (%)	100.0 (99.7)	98.3 (95.1)
$R_{\rm merge}$†	0.059 (0.375)	0.059 (0.375)
$\langle I/\sigma(I)\rangle$	36.8 (3.8)	23.6 (3.2)

† $R_{\rm merge} = \sum_{hkl}\sum_i |I_i(hkl) - \langle I(hkl)\rangle| / \sum_{hkl}\sum_i I_i(hkl)$, where $I_i(hkl)$ is the intensity of the ith observation and $\langle I(hkl)\rangle$ is the mean intensity of the reflection hkl.

2.3. X-ray diffraction study

All diffraction data for the bb' fragment and T3–bb' fragment complex crystals were collected under cryogenic conditions from crystals soaked in Paratone-N (Hampton Research) and cooled to 100 K in a stream of nitrogen gas. Diffraction images were collected using an ADSC Quantum 315 CCD detector at the BL38B1 station at SPring-8 and were processed and scaled using the *HKL*-2000 program package (Otwinowski & Minor, 1997).

3. Results and discussion

The bb' fragment crystal belonged to space group $C222$, with unit-cell parameters a = 94.8, b = 114.9, c = 182.9 Å. Assuming that there are four bb' fragments in the asymmetric unit, the Matthews coefficient was 2.25 Å^3 Da^{-1}, corresponding to a solvent content of 45.3% (Matthews, 1968). A total of 138 559 measured reflections in the resolution range 40–3.06 Å were merged to 36 262 unique reflections with an $R_{\rm merge}$ of 7.0%, a completeness of 100.0% and an $\langle I/\sigma(I)\rangle$ of 36.8. The corresponding values for the highest resolution shell were 3.17–3.06 Å, 3629, 43.3%, 99.7% and 3.8, respectively. The T3–bb' complex crystal belonged to space group $P2_12_12_1$, with unit-cell parameters a = 99.9, b = 184.5, c = 232.2 Å. Assuming that there are 16 T3–bb' complexes in the asymmetric unit, the Matthews coefficient was 2.41 Å^3 Da^{-1}, corresponding to a solvent content of 49.1% (Matthews, 1968). A total of 561 507 measured reflections in the resolution range 40–3.00 Å were merged to 161 916 unique reflections with an $R_{\rm merge}$ of 5.9%, a completeness of 98.3% and an $\langle I/\sigma(I)\rangle$ of 23.6. The corresponding values for the highest resolution shell were 33.11–3.00 Å, 15 639, 37.5%, 95.1% and 3.2, respectively. The data-processing statistics are shown in Table 1.

Structure determination by molecular replacement using the NMR structure of the bb' fragment of human PDI (PDB entry 2k18; Denisov *et al.*, 2009), which has a sequence identity of 93%, is currently in progress. In parallel, several phasing trials, *i.e.* the preparation of heavy-atom and SeMet derivatives, are also under way.

The synchrotron-radiation experiments were performed at BL38B1 of SPring-8 with the approval of the Japan Synchrotron Radiation Research Institute (JASRI; Proposal No. 2010B2011). This study was partially supported by a Grant-in-Aid for Scientific Research (B) from the Japan Society for the Promotion of Science, a Grant-in Aid from Hyogo Science and Technology Association and the Support Project to Assist Private Universities in Developing Bases for Research from the Ministry of Education, Culture, Sports, Science and Technology. This study was also partially supported by a Grant-in-Aid from Kwansei Gakuin University.

References

Darby, N. J. & Creighton, T. E. (1995*a*). *Biochemistry*, **34**, 11725–11735.
Darby, N. J. & Creighton, T. E. (1995*b*). *Biochemistry*, **34**, 16770–16780.
Denisov, A. Y., Maattanen, P., Dabrowski, C., Kozlov, G., Thomas, D. Y. & Gehring, K. (2009). *FEBS J.* **276**, 1440–1449.
Fu, X.-M., Wang, P. & Zhu, B. T. (2011). *Biochemistry*, **50**, 106–115.
Hashimoto, S., Okada, K. & Imaoka, S. (2008). *J. Biochem.* **144**, 335–342.
Hiroi, T., Okada, K., Imaoka, S., Osada, M. & Funae, Y. (2006). *Endocrinology*, **147**, 2773–2780.
Kemmink, J., Darby, N. J., Dijkstra, K., Scheek, R. M. & Creighton, T. E. (1995). *Protein Sci.* **4**, 2587–2593.
Kemmink, J., Dijkstra, K., Mariani, M., Scheek, R. M., Penka, E., Nilges, M. & Darby, N. J. (1999). *J. Biomol. NMR*, **13**, 357–368.
Matthews, B. W. (1968). *J. Mol. Biol.* **33**, 491–497.
Nguyen, V. D., Wallis, K., Howard, M. J., Haapalainen, A. M., Salo, K. E., Saaranen, M. J., Sidhu, A., Wierenga, R. K., Freedman, R. B., Ruddock, L. W. & Williamson, R. A. (2008). *J. Mol. Biol.* **383**, 1144–1155.
Obata, T. & Kubota, S. (2000). *Neurosci. Lett.* **296**, 41–44.
Okada, K., Imaoka, S., Hashimoto, S., Hiroi, T. & Funae, Y. (2007). *Mol. Cell. Endocrinol.* **278**, 44–51.
Otwinowski, Z. & Minor, W. (1997). *Methods Enzymol.* **276**, 307–326.
Primm, T. P. & Gilbert, H. F. (2001). *J. Biol. Chem.* **276**, 281–286.
Suzuki, T., Mizuo, K., Nakazawa, H., Funae, Y., Fushiki, S., Fukushima, S., Shirai, T. & Narita, M. (2003). *Neuroscience*, **117**, 639–644.
Tian, G., Xiang, S., Noiva, R., Lennarz, W. J. & Schindelin, H. (2006). *Cell*, **124**, 61–73.